A SIMPLIFIED MODEL FOR THE PREDICTION OF ARCJET PLUMES[1]

Duane A. Nelson
The Aerospace Corporation
P.O. Box 92957
Los Angeles, CA 90009-2957, USA

Yoshifumi Gotoh
Mitsubishi Electric Corp., Kamakura Works, JAPAN

Ideo Masuda
National Space Development Agency of Japan, Tsukuba, Ibaraki, JAPAN

Abstract

A procedure for the calculation of arcjet plumes which focuses on the primary performance parameters and hides complexity in a simplified model is presented. It is based upon a Monte Carlo method for rarefied flows because this is essential for accurate predictions of small rocket plumes. Calculations are compared to one another in a parametric sense and to recent experimental data. It is shown that the simplified procedure produces very good predictions for a 1.6 kW hydrazine arcjet plume.

Introduction

Spacecraft propulsion produces undesirable side effects consisting of forces, moments and heating due to plume impingement on various appendages. A typical plume analysis will involve aspects of thermochemistry, kinetics, continuum and rarefied fluid mechanics, heat transfer and mechanics. For an arcjet there are the additional complications of very high temperatures and electromagnetics.

For chemical thrusters there are well developed and generally available methods for all aspects of the problem but the same cannot be said for the arcjets. Typically the implementations of arcjet methods are available only to their developer and may not be complete enough for some applications. A good example would be the low power units rated at two kilowatts or less. Very little of the physics or chemistry will conform to an equilibrium model and rarefaction will be significant even within the nozzle flow.

It is a matter of our experience that small thrusters require a molecular method for analysis of the plume and the internal flow as well. The internal flow calculation should start near the nozzle throat at a somewhat subsonic condition with the Mach number in the range of 0.95 to 0.98. For an arcjet this is within the region of the arc and very complex physics are occurring. The objective of this paper is to show that some simple approximations will allow a reliable molecular analysis of the arcjet plume properties.

To our knowledge there is no prior work on prediction of arcjets plumes which could be applied to an impingement analysis. Prior molecular simulations have been for Hydrogen arcjet internal flow and nearfield plume properties[1].

Problem Description

The plume of a typical spacecraft thruster is largely rarefied. Molecular methods based upon a Monte Carlo algorithm is the correct way to compute the plume flowfield. Flow properties must be known or other boundary conditions prescribed over the whole surface of the computational domain. When flow properties are given it is usually necessary that local translational equilibrium prevails so that a Maxwellian velocity distribution can be employed. We have found that, for small thrusters, it is best to start the Monte Carlo solution near the nozzle throat because viscous effects are very strong and slip effects occur at the nozzle wall. For the arcjet, the throat region is at extremely high temperatures and electromagnetic phenomena are still important. However, a short distance downstream from the throat an essentially nonreactive flow is realized and the electric current is greatly reduced. From that point onward a model with translational, rotational and vibrational degrees of freedom will be all that is needed for calculation of the nozzle and plume flow.

There are reasons to consider the possibility of using the above model throughout the nozzle. In spite of physical complexity, the arcjet is a thermal engine which produces a given thrust and specific impulse for a given power input. It is expected that well chosen initial conditions at the throat can produce the expected performance at the sacrifice of some detail in that region. The small arcjets are very viscous in the nozzle and initial detail tends to be forgotten through diffusion. Moreover, chemical composition is essentially frozen throughout most of the nozzle and the plume. The principal parameters are the thrust, flowrate and overall chemical composition of the plume. Given these, the initial conditions near the throat are chosen as follows: (i.) a constant pressure, (ii.) a constant Mach number, somewhat less than one, (iii.) a uniform chemical composition determined by the overall composition of the plume and (iv.) a parametric representation of the temperature distribution with constants determined to match the known flowrate and specific impulse. It is possible to choose constants in such a way that flowrate remains constant while specific impulse is varied. The overall plume composition is uncertain without experimental data. In the present work such data was available but another composition was used based upon flowfield predictions provided by the arcjet manufacturer. Some parametric variation was also used to test the sensitivity of the results.

Approximate methods of plume analysis are generally based upon the plume farfield asymptote. In that limit the density varies inversely with the square of the distance from the centerline of the nozzle exit plane but shows a strong variation with the angle measured relative to the plume symmetry axis. Many implementations of this approach use a convenient, but arbitrary, angular distribution function and make use of isentropic relations to determine other flow properties from the density. These procedures are incorrect because of strong nonequilibrium plume expansion. Use of the Monte Carlo method (DSMC) developed by G. A. Bird [2] is the correct procedure and was used for this work to predict plume properties. From those, the farfield properties were easily determined. For the nonequilibrium flows the density varies as described above because it is required by mass continuity. Other property values such as velocity, various temperatures and composition tend to become constants independent of distance but show considerable variation with angle. The most important properties are the momentum flow per unit solid angle and energy flow per unit solid angle. The former determines impingement forces and the latter fixes heat transfer rates.

In what follows all plume results are expressed in the farfield interpretation.

Results and Discussion

Table 1, in two parts, gives a selection of the various cases considered in the analysis. All of the performance figures are calculated values except for the last row. For comparison, the manufacturer's specifications gives a thrust range from 0.225 to 0.246 N with corresponding specific impulse of 525 s and 512 s with an electric power input of 1.6 kW. These correspond to flowrates from 42.9 mg/s to 49.0 mg/s.

The first four rows show input data and performance results for calculations made to support an impingement analysis before experimental data was available. The species composition was based upon exit plane estimates provided by the arcjet manufacturer[3]. All of the remaining calculations used experimentally determined overall composition and peak temperatures closer to expected values in the arc. Case 8.1 does a very good job of matching the specification at the lowest rated thrust. The best match at the highest rated thrust is given by case 3 but note that the peak temperature is well below the expected value near ~40000 K.

Most of the last six cases describe variations made to seek better predictions of experimental results. Two of these show increased values of the anode wall temperature. The higher wall temperatures have a significant effect on specific impulse (compare cases 8.4, 8.5 and 8.7). The wall temperature effect will be considered again farther along. The nominal wall temperature is not shown but is not atypical of values that can be found in the literature and is well below the 2500 K value.

Case 8.7 provides a very good match to the experimental thrust and flowrate. Further discussion will follow but it is noted that the experimental thrust is indirectly determined by integration of measured plume properties. There were no measurements which allowed an estimate of the nozzle wall temperature and the value shown should not be considered as such. It is unusually high and close to the nozzle material melting temperature. However, it does help the prediction match data discussed below.

The main purpose of the plume prediction is to obtain accurate farfield representations of momentum and energy. This must be done in a simplified way, so knowledge of sources of error is essential. The basic hypothesis made herein is that matching thrust and flowrate (or specific impulse) should be the primary focus and that the details are secondary. To illustrate this, several comparisons from Table 1 are useful.

A flux per unit solid angle is defined by the relation

$$F_\phi=\rho V \phi r^2 \qquad (1)$$

where ρ is density, V is velocity, ϕ is unity for mass flux, V for momentum flux and $V^2/2$ + Ei for total energy flux and r is generally the distance from the centerline of the nozzle at the exit plane. In the farfield of a plume F_ϕ depends only on the angle relative to the nozzle centerline, θ. $F_\phi(\theta)$ gives a full description of each property, ϕ, when its angular distribution is known. The momentum flux is the most important plume property as it determines the impingement forces on a spacecraft. To verify our simplified model a comparison of F_v for nearly equal thrust will suffice. From the Table there are three good candidates; (i.) cases 2 and 8.1 (ii.) cases 4 and 8.4 and (iii.) cases 8.2 and 8.5.

Figures 1-3 show these results. In every case the angular distributions are very much alike and in two cases are nearly identical up to 120 degrees. The first case shows the largest differences of about ten percent. Considering the very large difference in the initial temperatures and the different composition this is very good agreement. Results in Figure 2 compare cases where thrust, and specific impulse are nearly the same but each has different initial temperatures and composition. This illustrates the point that thrust and specific impulse are the most important parameters and details of initial conditions are secondary. Differences in the energy flux (not shown) are noticeably larger due to the fact that one case includes vibrational degrees of freedom and the other does not. Figure 3 compares cases with similar thrust and composition. The specific impulse difference is significant because of differences in initial temperatures and the wall temperature. In spite of these differences the momentum flux distributions are nearly identical. The energy flux distributions (not shown) differ as expected primarily due to the specific impulse difference.

Further verification of the analytical method can be found in the experimental data of reference [4]. Case 8.7 matches the experimental conditions very well, as shown in Table 1. Figure 4 compares the analytical and experimental momentum flux distributions. The mass flux distribution is very similar. Up to about 50 degrees the prediction is in excellent agreement with the data. Thereafter, the data tend to fall above the prediction. One possible explanation for this is the finite vacuum-chamber pressure for the experiments. The predictions apply to a pure vacuum expansion. The behavior shown is known to be consistent with this interpretation.

Figures 5-7 provide a more detailed comparison of predictions and experimental data. The various properties are shown for each plume species and include mass flux, mean velocity and parallel temperature. The experiments measured the velocity distribution of each species along the direction primarily parallel to the mean velocity vector. In a rarefied flow the kinetic temperature is not a scalar but a vector, best resolved into components parallel and perpendicular to the mean velocity vector. It is this parallel kinetic temperature that is shown in Figure 7. The predictions are quite good for the heavier species but with the exception of the velocity they are only fair for the light species. Agreement with the velocities and temperatures required the very high wall temperature shown in Table 1 for this case. Unfortunately, the actual wall temperature during the experiments is unknown. It is conceivable that some other physics could be responsible for the data trends but the high wall temperature does very well in explaining the data and should not be discounted.

It is apparent from Figures 5 and 6 that the large deviation of the momentum flux of light species at large angles cannot be due to the differences in velocity and must be due to the density. This further suggests a background effect due to the imperfect vacuum of the experimental chamber. Although comparison of data and predictions at lower wall temperatures are not shown, they generally failed to predict the trend shown by the H atom velocity. The predicted magnitudes of velocity were generally much lower; up to 2000 m/s for H and 500 m/s for N2.

Summary and Conclusions

A simplified approach for the prediction of a low power, hydrazine arcjet plume has been shown to work extremely well by comparison of analytical studies and experimental data. Calculations must be carried out using a molecular method but the complications of nonequilibrium chemistry and electromagnetics can be avoided by choosing flow initial conditions at the nozzle throat that produce a specified thrust and flowrate (or specific impulse). These results for plume momentum and energy fluxes are insensitive to the initial species composition. The initial temperature distribution should be selected to match expected centerline and near wall values but the precise details are not important. Chemical reactions can be successfully ignored but the molecular model should contain vibrational degrees of freedom to better represent the energy flow.

Predictions of the variation of total momentum and energy flow in the plumes can be very accurate but details of properties of various plume species requires, at the very least, a knowledge of the nozzle wall temperature.

The model has not been tested for any but a hydrazine arcjet, where there are large differences in species molecular mass. Whether it would perform as well for an arcjet using a homonuclear diatomic species is unknown. It could not be applied directly to large arcjets because calculations starting at the nozzle throat would be much more computationally intensive and probably impractical.

References

[1] Boyd, I. D., "Monte Carlo Simulation of Nonequilibrium Flow in a Low Power Hydogen Arcjet", Physics of Fluids, Vol. 9, No. 10, 1997, pp. 3086 – 3095.

[2] Bird, G. A. , Molecular Gas Dynamics, Oxford University Press. London, 1976.

[3] Primex Aerospace Company, private correspondence.

[4] Pollard, J. E., Masuda, I., and Gotoh, Y., "Plume Mass Spectrometry and Calorimetry with a Hydrazine Arcjet Thruster", 26th International Electric Propulsion Conference, Kitakyushu, Japan, 1999.

Case#	Thrust, N	Flowrate, kg/s	T max, K	T min, K	V max, m/s	V min, m/s	Isp, m/s
1	0.216	4.52e-05	6000	6000	2500	2500	4788
2	0.223	4.54e-05	20000	3560	2500	2500	4912
3	0.243	4.76e-05	24000	2350	5000	1900	5107
4	0.245	4.54e-05	42000	1900	6614	1407	5410
8.1	0.220	4.22e-05	44000	1240	6937	1136	5214
8.2	0.253	4.98e-05	40000	1128	6614	1083	5090
8.4	0.247	4.59e-05	48400	1365	7284	1193	5389
8.5	0.257	4.59e-05	48400	1365	7284	1193	5608
8.6	0.282	4.96e-05	42000	1900	6614	1407	5689
8.7	0.266	4.60e-05	48400	1365	7284	1193	5783
exp	0.266	4.64e-05					

(a)

Case#	Isp, s	N2, mole %	N, mole %	H2, mole %	H, mole %	T wall, K
1	488	26.67	0	33.33	40	
2	501	26.67	0	33.33	40	
3	521	26.67	0	33.33	40	
4	552	26.67	0	33.33	40	
8.1	532	25.75	6.28	50.96	17.01	
8.2	519	25.75	6.28	50.96	17.01	
8.4	550	25.75	6.28	50.96	17.01	
8.5	572	25.75	6.28	50.96	17.01	2500
8.6	580	25.75	6.28	50.96	17.01	
8.7	590	25.75	6.28	50.96	17.01	3500
exp	585	25.75	6.28	50.96	17.01	???

(b)

Table 1: Performance and Initial Conditions

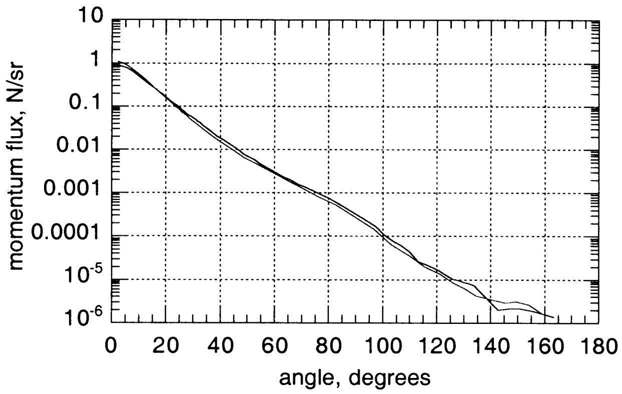

Figure 1: Comparison of Cases 2 and 8.1

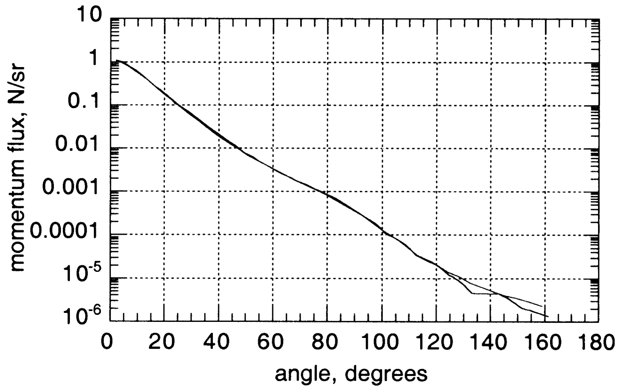

Figure 2: Comparison of Cases 4 and 8.4

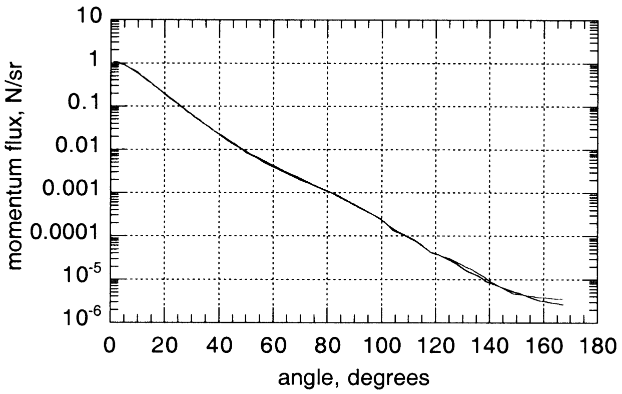

Figure 3: Comparison of Cases 8.2 and 8.5

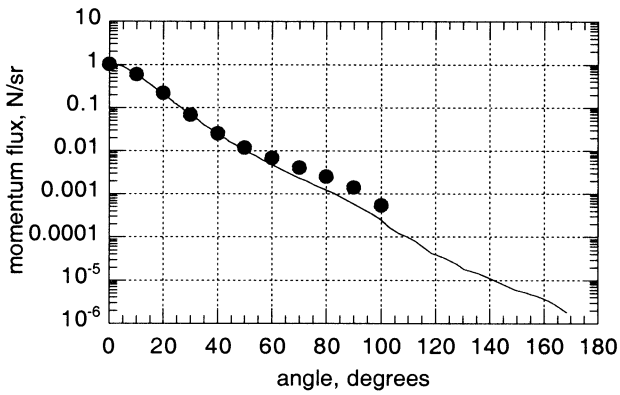

Figure 4: Comparison of Cases 8.7 and exp

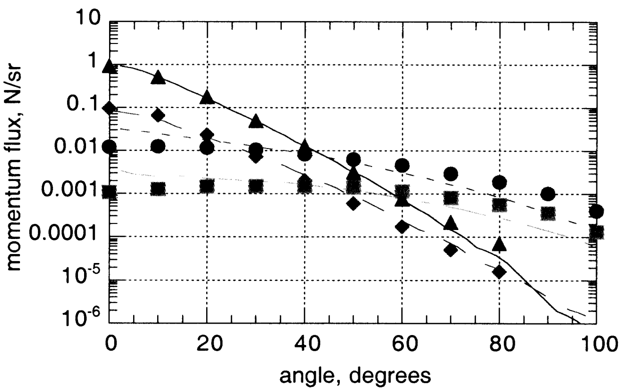

Figure 5: Prediction 8.7 and Experiment
N2, N, H2, H from top to bottom at left

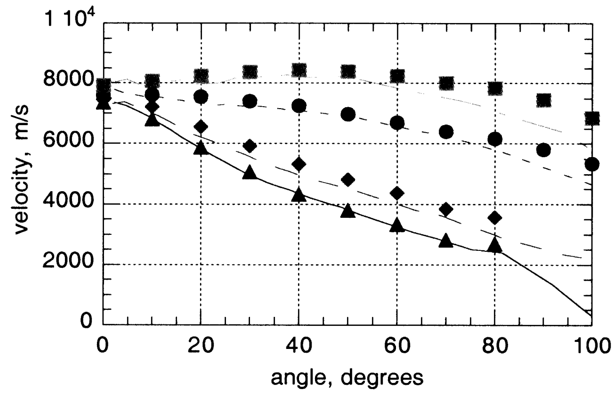

Figure 6: Prediction 8.7 and Experiment
N2, N, H2, H from bottom to top

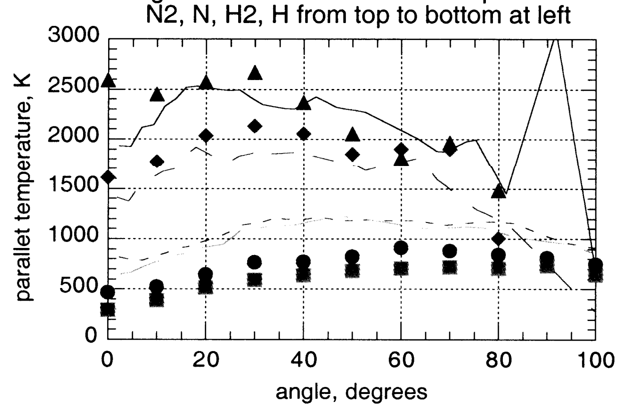

Figure 7: Prediction 8.7 and Experiment
N2, N, H2, H from top to bottom